Aspects Regarding the Operation of Ventilation and Air Conditioning Systems for Industrial Halls

Monica-Adela Enache*, Elena-Mihaela Enache† and Mara Pauliuc†

* University of Craiova/ Faculty of Electrical Engineering, Craiova, Romania, menache@em.ucv.ro

† "Ion Mincu" University/Faculty of Architecture, Bucharest, Romania, elena.enache2305@gmail.com

***Abstract* – This paper emphasizes, once again, the importance of ventilation systems for ensuring thermal comfort in industrial spaces. For this purpose, a dynamic fault regime of variable reluctance synchronous motors (RSM) used to drive such systems (case of occurring an accidental resistive torque) is analyzed from a theoretical point of view (with experimental confirmation). At the beginning, an introduction in the issues of the paper is made. A brief bibliographic analysis and some relevant images regarding the air flow driven by industrial ventilation and air conditioning systems are presented. In order to analyze dynamic regimes of RSM, a Matlab program was carried out, by using a mathematical model written in the two axes theory. A series of graphs have been obtained by running it for a specific case; they emphasize the evolution over time of the main electrical, magnetic and mechanical quantities of the motor. There have been obtained different evolutions of the operation points in various coordinates (phase current, longitudinal and transverse currents of the stator and rotor, magnetization current, magnetization flux, magnetization flux components, torque and speed). The graphs obtained led to a series of relevant conclusions regarding the behavior of the driving motor of the installation (conclusions regard the way in which an increase in the resistant torque influences the values and durations of the analyzed dynamic quantities). The paper ends with Acknowledgment and the corresponding References.**

Cuvinte cheie: *sisteme de ventilatie, hale industriale, reluctance synchronous motor, dynamic regime, modelation, simulation, test.*

Keywords: *ventilation systems, industrial halls, reluctance synchronous motor, dynamic regime, modeling, simulation, test*.

I. INTRODUCTION

The problem of designing green industrial building is a nowadays problem that represents a challenge for any architectural office [1], [2], [3] and [4].

An important component of this design is the appropriate sizing of ventilation and air conditioning equipments, which ensure appropriate thermal comfort for people working in these buildings [5], [6], [7] and [8].

This paper aims at analyzing a relevant aspect regarding the behavior of an important component of such an installation - the driving motor (the problem also presented in [9], [10], [11] and [12]).

From the multitude of driving motors, a modern, simple, cheap and very reliable motor was chosen, the reluctance synchronous motor (RSM).

This way, this paper is also a natural continuation of the initial analysis presented in [13].

When it comes to the design of ventilation and air conditioning systems for industrial halls, the basic principles of fluid mechanics always are applied, irrespective of the specific requirements for the hall temperature.

These principles have an impact on the design and technology of ventilation installation, which means that they also influence operating costs.

For example, a vertical temperature gradient should be oriented to keep heat loss to a minimum, keeping the vertical temperature rise as low as possible, especially in the upper area of the hall.

A manner of doing this, is to maintain a maximum air circulation in the aisle.

The flow conditions will be optimized, for example, by using grid shelving systems that are permeable and have a generous gap between them and the floor.

The specific flow features of the torsion air distributors - including the patented Hoval Air-Injector - ensure that the air in the storage halls is distributed according to requirements.

In heating mode, a highly concentrated air flow is emitted at high speed from the distributor and a negative pressure difference occurs around the air column (Bernoulli distribution).

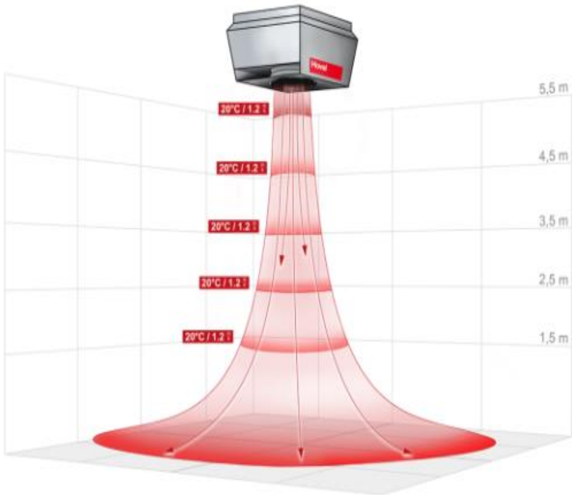

Fig. 1. Vertical airflow [14].

As a result, ambient air moves from the ceiling area and, to a less extent, from the upper shelves towards the air flow (Fig. 1).

As the penetration depth increases, the airflow is reduced, the surrounding negative pressure decreases, and the ambient air is induced (Fig. 2).

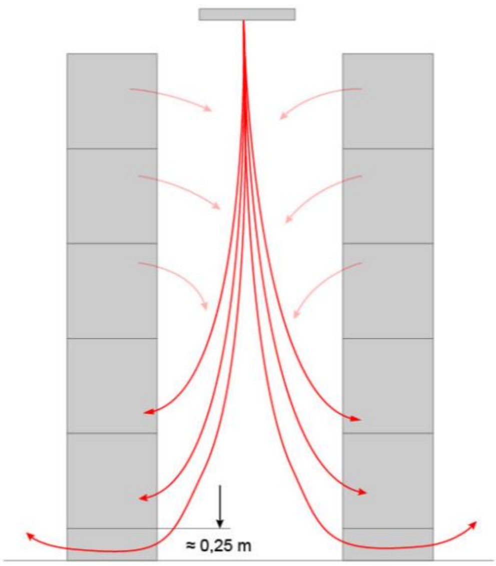

Fig. 2. Airflow through the aisle: air supplied vertically from above allows a low temperature gradient over the entire height. In a hall that is between eight and twenty meters high, the values will typically be somewhere between 0.15 Kelvin and 0.25 Kelvin [14].

The flow then reaches the shelves below.

In order to pass the flow efficiently to next shelves, a gap of 0.2 to 0.3 meters (m) must be left between the floor and the shelf.

The improved air distribution makes possible to optimize the flow for one, two or three aisles, with a series of air passages.

The rows of shelves restrict the symmetrical rotating flow of the torsion air distributors.

The fronts of the rows of shelves act as walls as regards the air flow, causing air jets on the surface of the walls (Coanda effect).

These have a wider coverage than open jets (Regenscheit formulation) and a higher installation height than in the case of free flow distribution.

The value can reach up to 1.5 m.

II. MATHEMATICAL MODEL

The present paper is a normal continuation of those presented in [13].

The starting point will be the mathematical model presented in [13], where it will be taken into account that the RSM has no excitation winding.

Thus, the mathematical model written in the fixed reference frame with respect to the rotor is obtained:

$$
\begin{aligned}
u_d - R_s i_d &= \frac{d\psi_d}{dt} - \omega\psi_q \\
u_q - R_s i_q &= \omega\psi_d + \frac{d}{dt}\psi_q \\
-R_D i_D &= \frac{d\psi_D}{dt} \\
-R_Q i_Q &= \frac{d\psi_Q}{dt}
\end{aligned}
\tag{1}
$$

where:

$$
\begin{aligned}
\psi_d &= L_d i_d + L_{md} i_D \\
\psi_q &= L_q i_q + L_{mq} i_Q \\
\psi_D &= L_{md} i_d + L_D i_D \\
\psi_Q &= L_{mq} i_q + L_Q i_Q
\end{aligned}
\tag{2}
$$

Substitute (2) into (1). We obtain:

$$
\begin{aligned}
u_d - R_s i_d + \omega L_q i_q + \omega L_{mq} i_Q &= L_d \frac{di_d}{dt} + L_{md}\frac{di_D}{dt} \\
u_q - R_s i_q - \omega L_d i_d - \omega L_{md} i_D &= L_q \frac{di_q}{dt} + L_{mq}\frac{di_Q}{dt} \\
-R_D i_D &= L_{md}\frac{di_d}{dt} + L_D \frac{di_D}{dt} \\
-R_Q i_Q &= L_{mq}\frac{di_q}{dt} + L_Q \frac{di_Q}{dt}
\end{aligned}
\tag{3}
$$

To these relations is added the equation of motion:

$$
\frac{3}{2} p\left(\psi_d i_q - \psi_q i_d\right) - m_r = \frac{J}{p}\frac{d\omega}{dt}, \tag{4}
$$

respectively:

$$
\frac{3}{2} p\left(L_d i_d i_q + L_{md} i_D i_q - L_q i_q i_d - L_{mq} i_Q i_d\right) - m_r = \frac{J}{p}\frac{d\omega}{dt}. \tag{5}
$$

The meanings of the notations are as detailed in [13].

III. SIMULATIONS

With the help of this mathematical model, a Matlab program was created. This Matlab program developed for analyzing a particular fault regime has been used: an increase in the shaft resistant torque value. The simulation results are presented in Fig. 3.

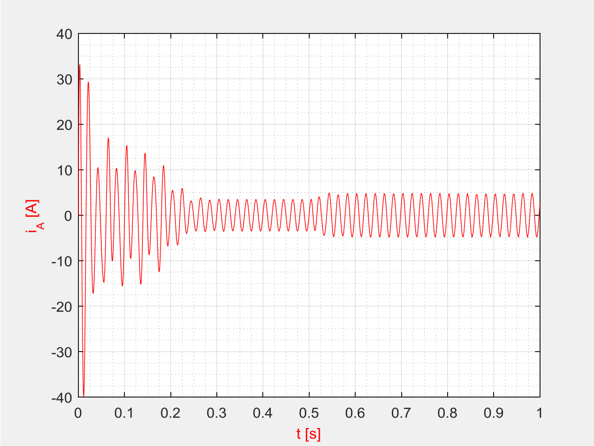

a)

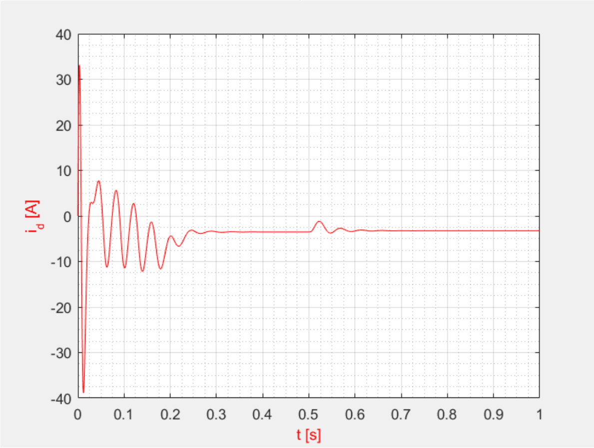

b)

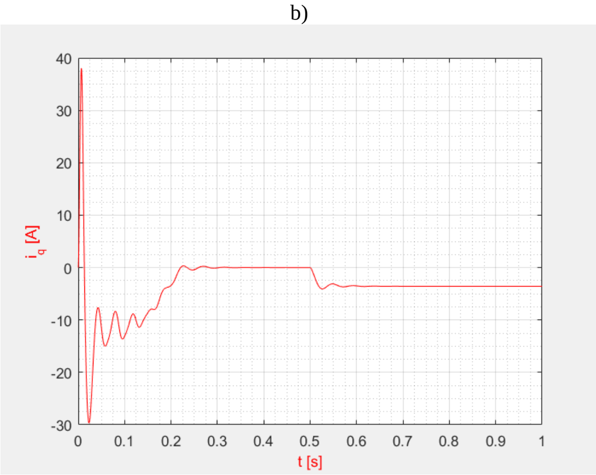

c)

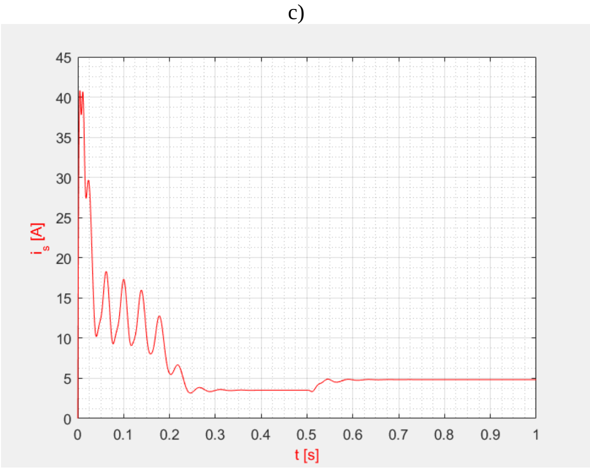

d)

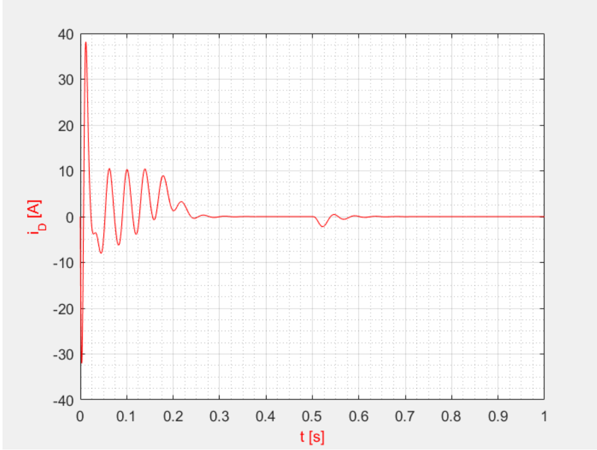

e)

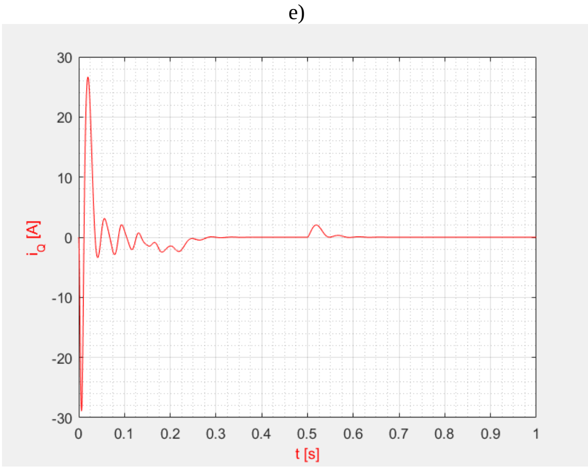

f)

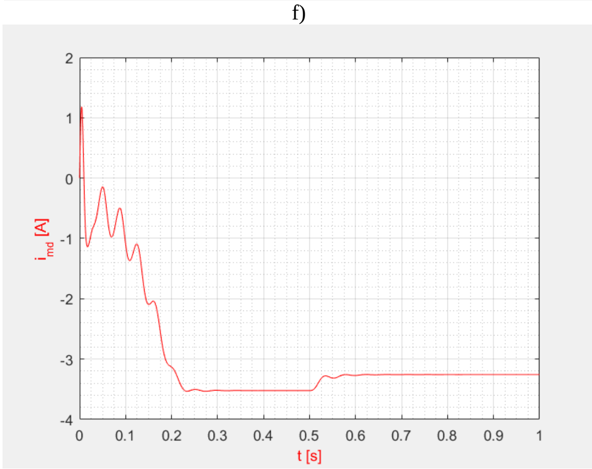

g)

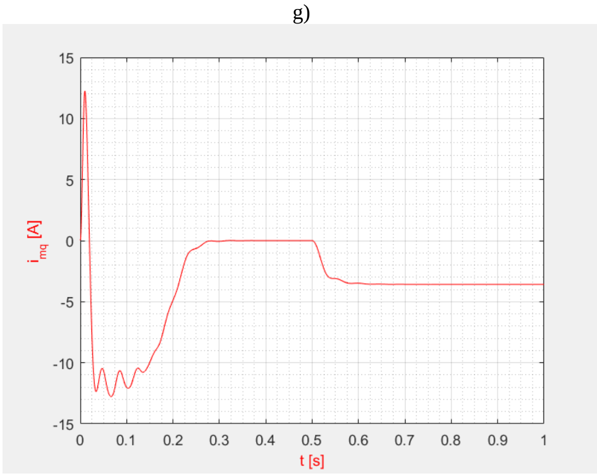

h)

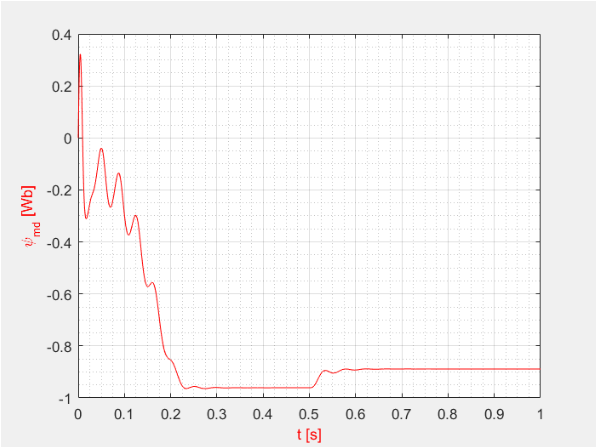

i)

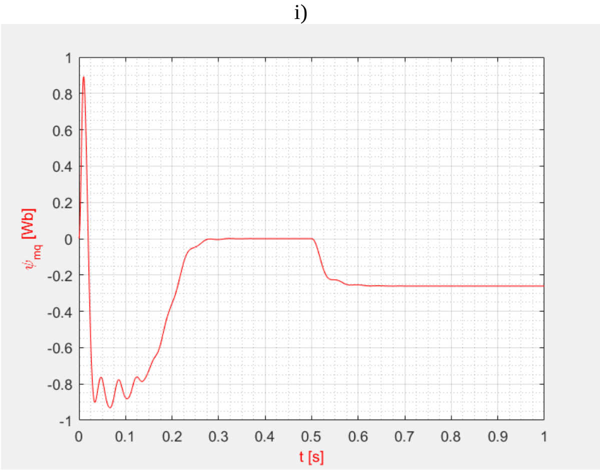

j)

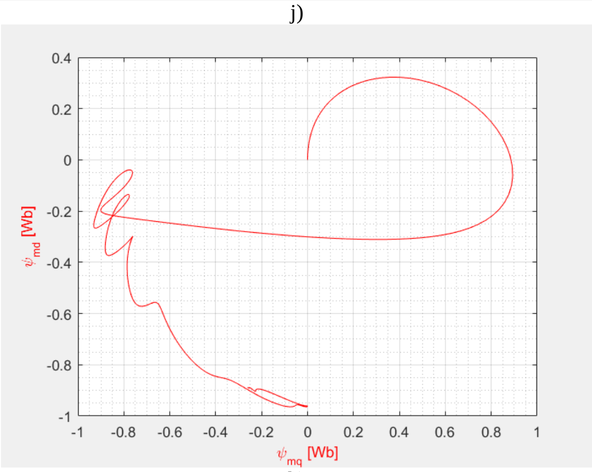

k)

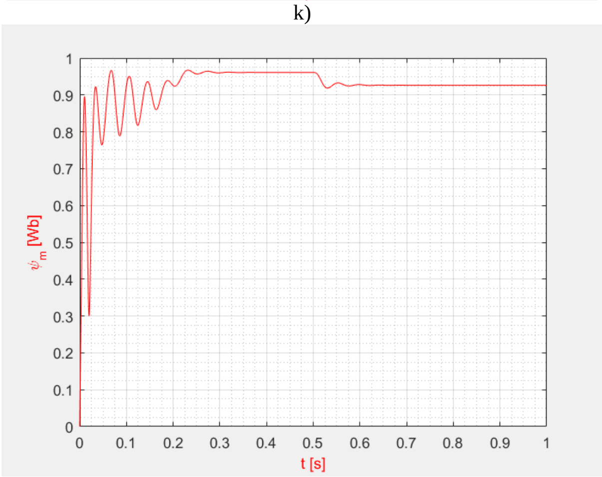

l)

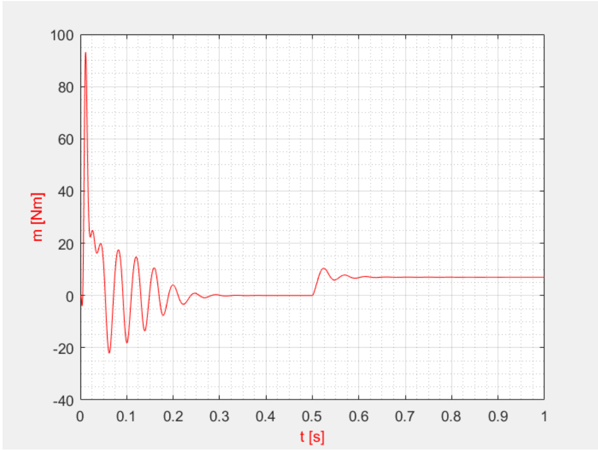

m)

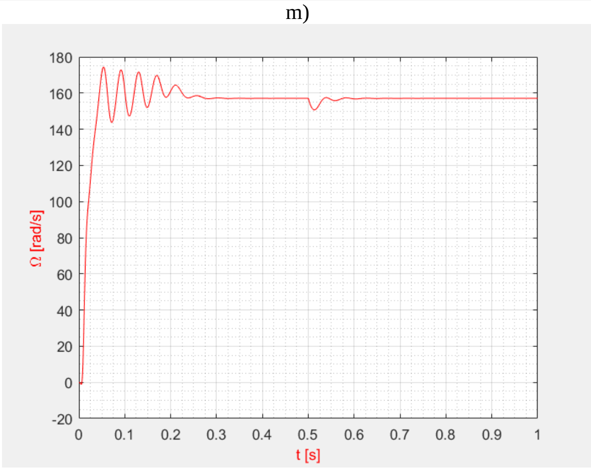

n)

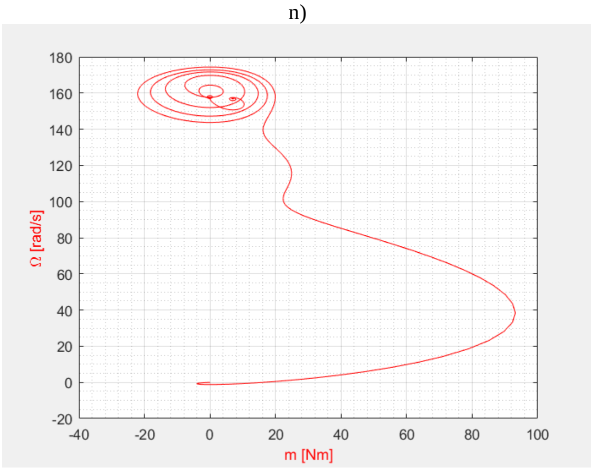

o)

Fig. 3. The characteristics obtained for the case of increasing the value of the resistant torque to 7.6 Nm after 0.5 s from starting.

The same motor as in [13] was used. The simulations were carried out for an motor rated as follows:

R_s = 3.77 Ω, R_D = 1.5 Ω, R_Q = 4.5 Ω, $L_{s\sigma}$ = 0.0081 H, $L_{D\sigma}$ = 0.0059 H, $L_{Q\sigma}$ = 0.0067 H, L_d=0.281 H, L_q=0.081 H; U = 220 V, p = 2, J=0.008 kg.m^2.

The graphs depicted in Fig. 3 have been obtained by running the program (the resistant torque increases from 0, initially, to 7.6 Nm).

IV. Experimental Determinations

The electrical diagram of the measurement system is shown in figure 4.

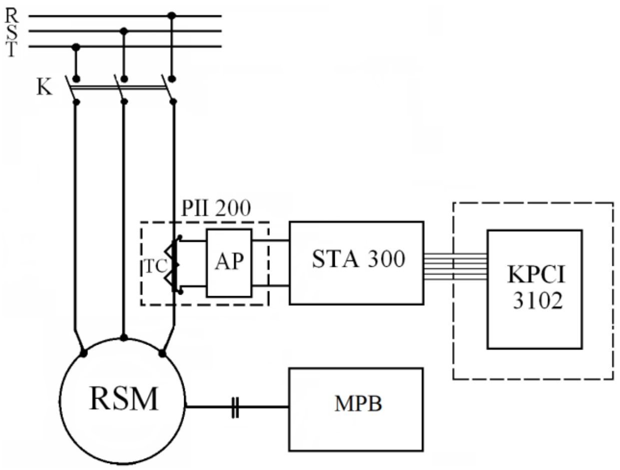

Fig. 4. Electrical diagram.

The meanings of the notations used are as follows:

- RSM - reluctance synchronous motor;
- MPB - magnetic powder brake;
- PII 200 - current transformer with adaptation block;
- STA 300 - connection block;
- KPCI 3102 - data acquisition board.

A magnetic powder brake [15] was used to load the motor.

It allows the resistive torque to be varied up to 10 Nm. A control block is used to change the torque.

Fig. 5. Magnetic powder brake [15].

The experiments consisted in acquiring the current variations for a steady-state of the RSM, for two concrete situations:

- the steady-state operation at 0 Nm (Fig. 6);

- the steady-state operation at 7.6 Nm (Fig. 7).

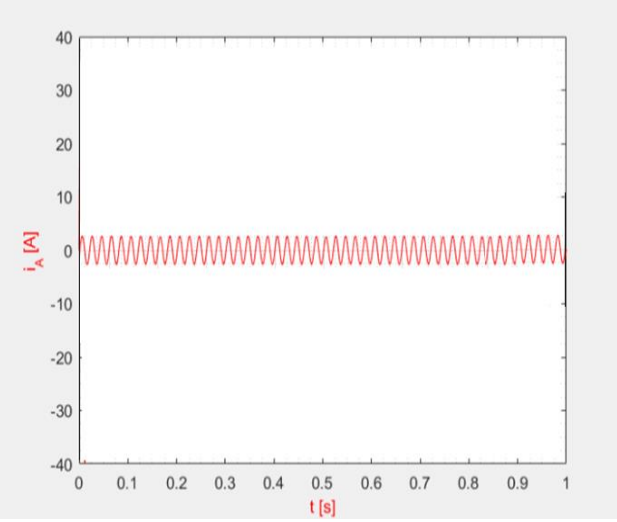

Fig. 6. The variation of the phase current, in case of steady-state operation, at 0 Nm.

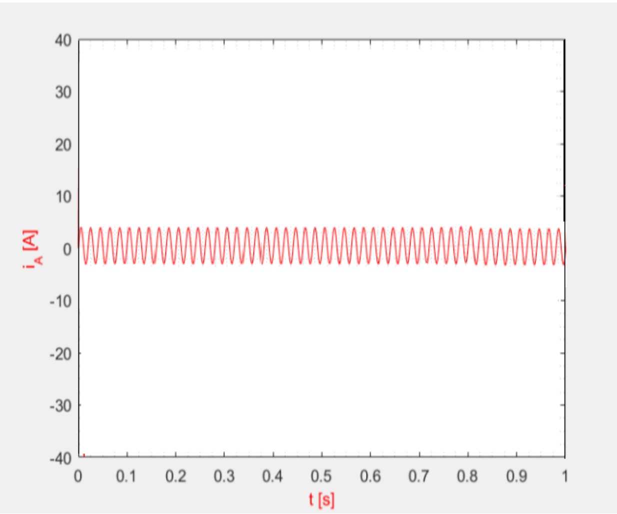

Fig. 7. The variation of the phase current, in case of steady-state operation, at 7.6 Nm.

Comparing these results with those depicted in Fig. 3.a (zone 0.3-0.5 s and zone 0.7-1 s), it is found that they are almost identical, which confirms the validity of the simulations (at least in steady state).

V. Conclusions

This paper presents a series of simulations that emphasize dynamic regimes of RSM, in case of certain external disturbances (an increase in the resistant torque).

Some of the conclusions obtained by analyzing the graphs presented above are presented below:

- occurring a resistant torque jump leads to an increase in the phase current;

- the current i_s also increases in the new steady state;

- after a short mechanical shock, occurred when the load was applied, the motor works stably at a slightly lower speed than the initial one;

- the motor has two stable operation points, corresponding to the two steady states (emphasized in the Ω=f(m) coordinates).

The conclusions were indirectly confirmed by previous experimental determinations.

ACKNOWLEDGMENT

Source of research funding in this article: Research program of the Electrical Engineering Faculty Craiova and the Faculty of Architecture Bucharest (financed by the University of Craiova).

Contribution of authors:

First author – 55 %;
First coauthor – 25 %;
Second coauthor – 20 %.

Received on September 7, 2024
Editorial Approval on November 25, 2024

REFERENCES

[1] H. Wang and W. Wang, “Optimization algorithm of green building landscape space environment based on geographic information system”, *2024 International Conference on Telecommunications and Power Electronics (TELEPE)*, Frankfurt, Germany, 2024, pp. 897-901.

[2] P. Zhang, “Research on the use of BIM technology in green building design based on neural network learning”, *IEEE Access*, Volume 12, 2024, pp. 94784-94792.

[3] Y. Zhang and X. Ren, “Research on green public building design based on computer 3D image vision technology”, *2023 IEEE International Conference on Sensors, Electronics and Computer Engineering (ICSECE)*, Jinzhou, China, 2023, pp. 970-974.

[4] C. Rao, “Optimal design of green building based on Digital Media Technology”, *2022 International Conference on Artificial Intelligence in Everything (AIE)*, Lefkosa, Cyprus, 2022, pp. 357-361.

[5] H. Zhou, Z. Li, Y. Liu, L. Mei, W. Lu, and J. H. Air, “Conditioning system design of power data center based on automatic control technology”, *2024 IEEE 2nd International Conference on Image Processing and Computer Applications (ICIPCA)*, Shenyang, China, 2024, p.1-4.

[6] U. Chowdhury, J. Rodriguez, M. Tradat, Q. Soud, S. Wallace, and D. O"Brien, “Acoustics analysis of air and hybrid cooled data center”, *2024 23rd IEEE Intersociety Conference on Thermal and Thermomechanical Phenomena in Electronic Systems (ITherm)*, Aurora, CO, USA, 2024, pp. 1-11.

[7] Z. Z. Bin Zainudin, S. H. Binti Yusoff, T. S. Gunawan, S. Y. Mohamad, I. J. Chowdhury, and S. N. Mohd Sapihie, “Load forecasting for air conditioning systems using linear regression and artificial neural networks”, 2024 IEEE 10th International Conference on Smart Instrumentation, Measurement and Applications (ICSIMA), Bandung, Indonesia, 2024, pp. 234-239.

[8] J. Han, G. Zhang, Z. Ye, Z. Fu, N. Zhao, and S. Wang, “Pole pairs identification for sensorless permanent magnet single-rotary air-conditioning compressor”, 2024 IEEE 19th Conference on Industrial Electronics and Applications (ICIEA), Kristiansand, Norway, 2024, pp. 1-6.

[9] J. Yi, C. Li, D. Zhang, X. Li, M. Jiang, and H. Zhao, “A fast and accurate loss model of converter-fed induction motor in central air-conditioning system”, *IEEE Transactions on Power Electronics*, Volume: 38, Issue: 3, March 2023, pp. 3689-3699.

[10] G. Balasubramanian, P. Chandrasekar, and S. A. Alexandar, “Variable frequency drive operated air blower in air handling unit of heating, ventilation and air conditioning systems”, *2022 IEEE Delhi Section Conference (DELCON)*, New Delhi, India, 2022, pp. 1-7.

[11] H. Hou, W. Yao, and W Zhang, “A novel control strategy of single phase brushless dc motor for automotive air conditioning”, *2016 IEEE Vehicle Power and Propulsion Conference (VPPC)*, Hangzhou, China, 2016, pp. 1-5.

[12] S. Kikuchi, A. Takahashi, H. Mikami, S. Wakui, H. Kou, K. Tanaka, “Development of self-starting permanentmagnet synchronous motors for compressor drives”, *2009 International Conference on Electrical Machines and Systems*, Tokyo, Japan, 2009, pp. 1-6.

[13] M. A. Enache, E.-M. Enache, and M. Pauliuc, “Simulations and tests regarding the operation of air heaters for industrial buildings”, *Annals of the University of Craiova, Electrical Engineering Series*, 2024, in press.

[14] https://www.hoval.ro/blog/ro/sisteme-de-ventilatie-industriala-si-climatizare-hale.

[15] https://roitzheim-werkzeugmaschinen.de/LN-Lucas-Nuelle-Magnetpulverbremse-Steuergeraet-Set-SE-2662-5R-und-SE-2662-5S-gebraucht_1.